Eighteen Months of Continuous Near-surface Monitoring with DAS Data Collected Under Stanford University

Eileen R. Martin

ABSTRACT

We use ambient noise interferometry on data recorded by a distributed acoustic sensing (DAS) array to extract signals mimicking active source surveys without the cost and permitting requirements of a traditional active survey for geotechnical characterization. Between September 2016 and March 2018, we passively recorded DAS data on an array of fibers in existing telecommunications conduits under the Stanford University campus. We analyze time-lapse changes in the ambient noise field throughout campus and observe diurnal, weekday/weekend, and some annual variation trends. We calculate noise correlation functions (NCFs) throughout the 18 months of recording to test whether the array's NCFs were sensitive to near-surface velocity changes tied to seasonal saturation cycles. During rainier winter months, we see higher signal-to-noise ratios (SNR) in one-bit cross-correlations. To understand whether temporal changes in the ambient noise field could cause spurious changes in NCFs, we compare two methods for calculating monthly NCFs and their resulting dispersion images. Evidence does not suggest that the array detects a velocity shift correlated to saturation changes, but it is possible SNR of NCFs at far offsets may provide a qualitative indicator of saturation.

BACKGROUND AND PRIOR WORK

For the purpose of near-surface characterization, including earthquake hazard analysis, on the Stanford campus, I am interested in processing ambient noise to avoid the cost, time and permitting requirements involved in active surveys. However, the Stanford campus displays a wide range of natural and anthropogenic noise sources which may not always be ideally distributed. Here, I analyze changes in the ambient noise field and NCFs throughout the first 555 days of data.

Ambient noise interferometry has successfully been used with point sensors to create data mimicking active surveys at the scale of a city (Chang et al., 2016) and time-lapse surveys at the reservoir scale (de Ridder, 2014). Further, groundwater changes in California have been observed over a larger scale using frequencies below 2 Hz through ambient noise interferometry of broadband seismometer data (Clements

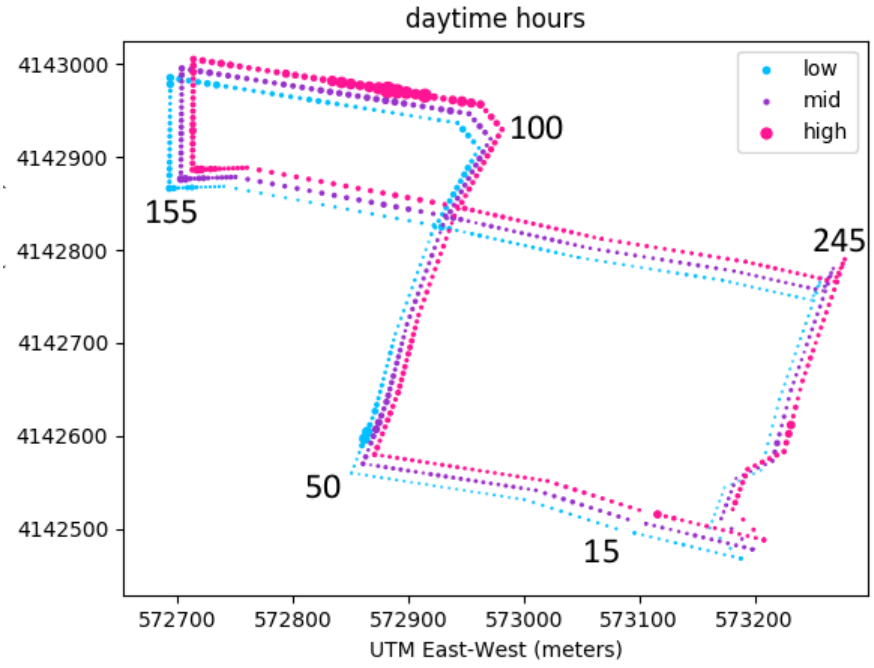

(a)

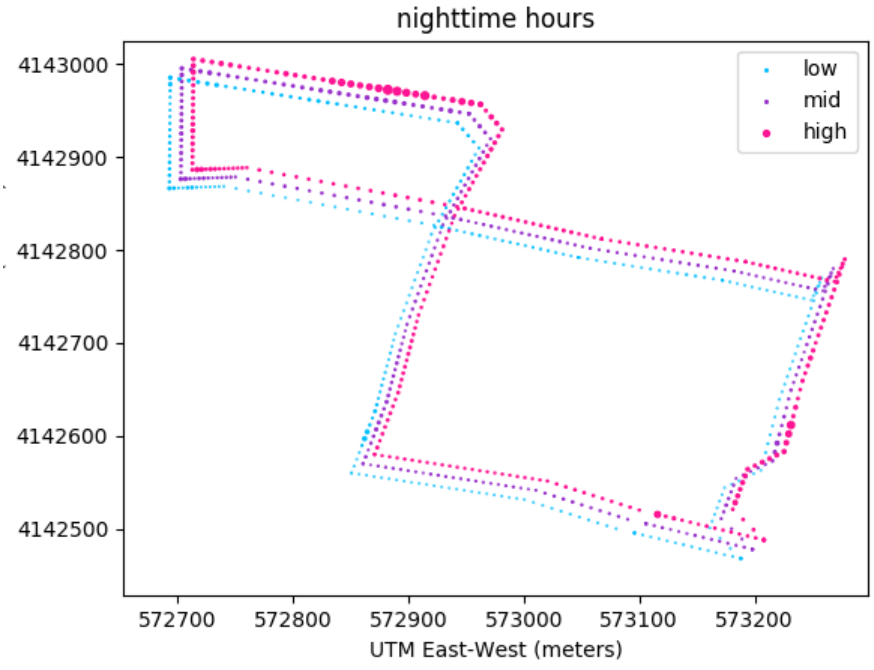

(b)

Figure 1: At each channel, the marker radius is proportional to the average spectral amplitude within three frequency ranges: 0.5-2.0 Hz (low, blue), 2.0-8.0 Hz (mid, violet) and 8.0-24.0 Hz (high, pink) average spectral amplitude. These are averaged over 18 months, separated into (top) daytime UTC 14:00 to 05:59, and (bottom) nighttime UTC 06:00 to 13:59. Several channel numbers are marked for reference. [**CR**]

and Denolle, 2017). Cross-correlations of data from a trenched DAS array recording a repeatable active source have indicated velocity changes on rainy days (Ajo-Franklin et al., 2017). Further, ambient noise interferometry at a trenched DAS array crossing a section of permafrost during an active thaw experiment shows a drop in velocities of NCFs as thawing occurred (Lindsey et al., 2017). Previously at the Stanford array, it has been observed that coherent NCFs can be extracted even between non-collinear channels, and those NCFs converge in most places within approximately one week (Martin et al., 2018). Given these studies, it is natural to wonder whether it is possible to observe velocity shifts tied to annual variations in saturation using ambient noise recorded here.

Inferring time-lapse velocity changes from ambient noise interferometry in an urban area is difficult because: NCF artifacts may be introduced by repeating noise sources that are not independent of each other (Martin et al., 2016), and changes in the amplitude spectrum or spatial distribution of the ambient noise field between epochs may introduce false apparent velocity changes in NCFs (Zhan et al., 2013). In both cases, the use of cross-coherence can reduce these effects (Martin et al., 2016; Daskalakis et al., 2016). However, the whitening process in cross-coherence may keep us from studying the dependence of NCF sensitivity on geometry within different frequency bands (Martin and Biondi, 2017), so I have previously focused on analysis of one-bit cross-correlations (Martin et al., 2016). In this study, I analyze changes in the ambient noise field, and compare time-lapse changes in NCFs calculated through one-bit cross-correlation and cross-coherence, as well as tracking the stability of dispersion curve picks.

SPATIO-TEMPORAL VARIATION OF AMBIENT NOISE

For each minute of data, I calculated each channel's amplitude spectrum, then averaged over each hour. As seen in Figure 1, there is more energy in the frequency ranges above 2 Hz, which tends to be anthropogenic noise. This can potentially cause issues because anthropogenic noise sometimes violates the assumption underlying ambient noise theory: that the ambient noise field is made of independent, uniformly distributed noise sources. The loudest area of the array, the north edge, is along a main campus road, and particularly during the daytime this area suffers from increased traffic, and construction activity. Daily traffic patterns are not necessarily a problem in monthly time-lapse ambient noise interferometry if they are consistent month-to-month.

In addition to diurnal trends, there is a secondary trend: weekend days are much quieter than weekend days, as evidenced by the regular dips in energy above 2 Hz in Figure 2. The typical trend is that areas with more vehicular traffic, including channel 75, show stronger diurnal and weekly trends and less change over the course of the year. Channels in quieter pedestrian-only alreas, including channel 255, show significant annual variability in energy above 2 Hz: quietest in the summer months and loudest in the winter (peak is around February each year). Because the farthest north

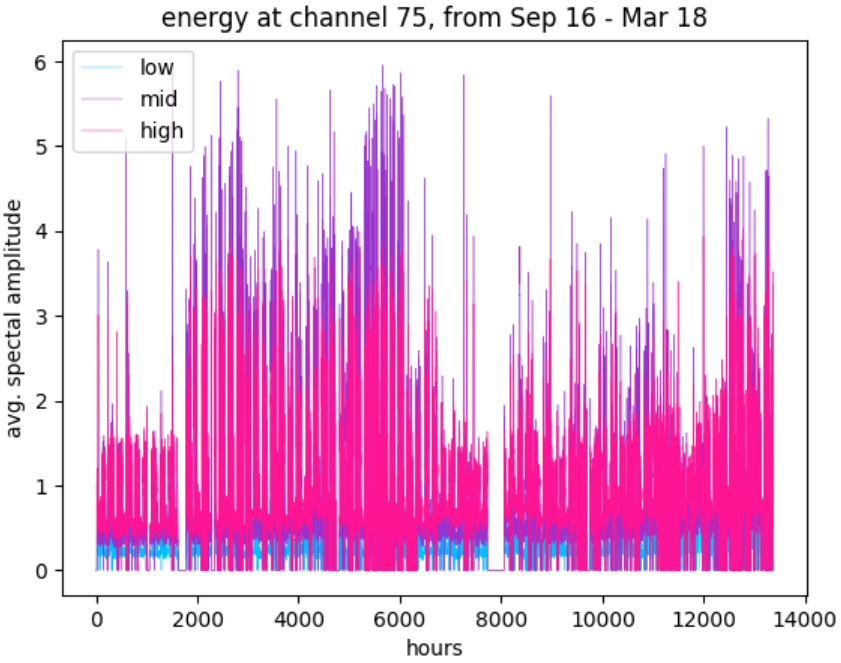

(a)

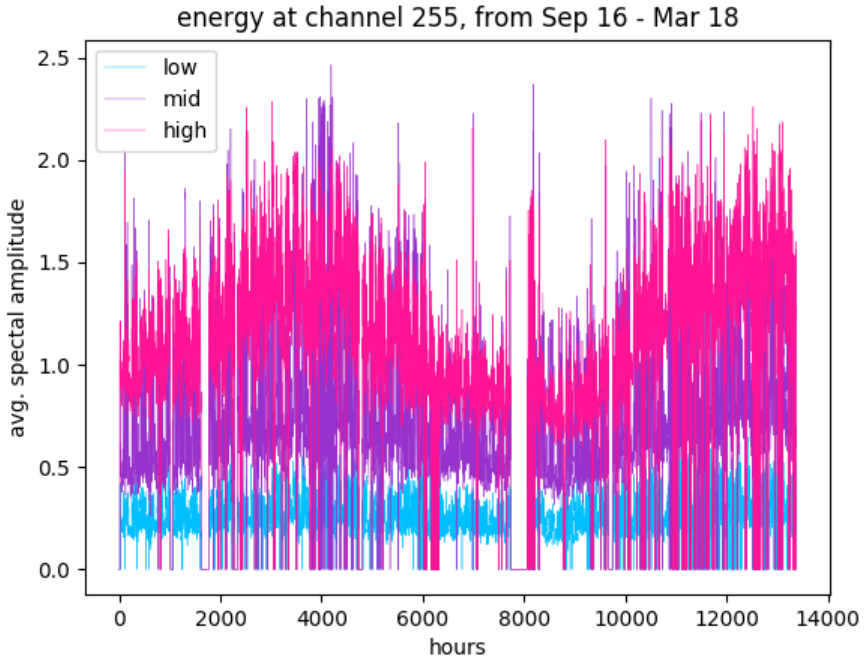

(b)

Figure 2: The hourly average spectral amplitudes are plotted for channels 75 (top) and 255 (bottom) in three frequency bands: 0.5-2.0 Hz (low, blue), 2.0-8.0 Hz (mid, violet) and 8.0-24.0 Hz (high, pink). In areas with more cars, including ch. 75, there is little seasonal variability, but pedestrian-only areas like ch. 255 show loud winters and quiet summers. [**CR**]

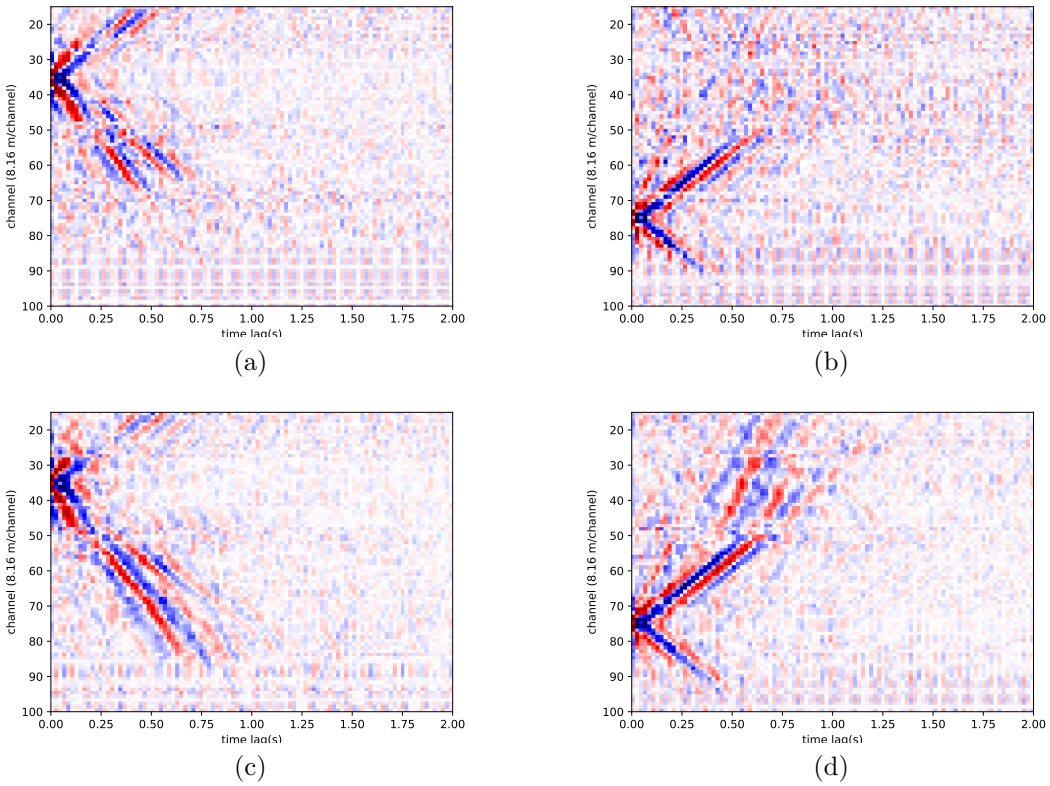

Figure 3: One-bit cross-correlations of ch. 15-100 with 35 (left) and 75 (right) in Sep. 2016 (top) and Mar. 2017 (bottom) show better SNR in March when the ground is more saturated. [**CR**]

and west lines (channels 100 to 165) are particularly affected by vehicle noise, and the southeast corner (channels 270 to 287) are particularly affected by reverberations of waves off two large building basements (Martin et al., 2017), it is unclear whether a coherent signal can be extracted so the treatment of these receivers is beyond the scope of this effort.

PROCESSING NOISE CORRELATION FUNCTIONS

One-bit cross-correlation is computationally cheap and should theoretically converge to NCFs that reflect information about attenuation and frequency-dependent geometric sensitivity of DAS NCFs. But these NCFs can demonstrate artifacts due to our non-ideal ambient noise field. Thus, I decided to calculate both the one-bit cross-correlation and the cross-coherence to understand whether velocity changes were robust to processing decisions, particularly in the presence of changing anthropogenic noise sources near the array. The aim of cross-coherence is reducing false velocity changes due to spectral amplitude shape differences over time (Zhan et al., 2013). Further, when dispersion analysis of cross-coherence results matches one-bit cross-correlation results, it may support the use of those one-bit cross-correlation NCFs for attenuation and frequency-related geometry sensitivity analysis.

For each one-minute window, I performed one-bit cross-correlation and cross-coherence for each receiver pair. For each hour, I stored the average one-bit cross-correlation and cross-coherence for each channel pair. I then calculated the monthly averages. First, I averaged the one-bit cross-correlations normalized by their L_2 norms. The resulting NCFs appear to have stronger extracted signals during the rainy winter months than dry summer and early fall months, as seen in Figure 3 for two orthogonal fiber lines reacting to two different virtual sources (one on each line) averaged over one week. This change is clearer at distances longer than 200 meters.

By using the L_2 norm, I de-emphasize hourly correlations with a concentrated wavelet and strong peak, making all monthly estimates noisier. Thus, in Figure 4 I show NCFs normalized by their L1 norm before monthly averaging to reduce this noise-quality difference and focus primarily on any velocity changes that may be present. To simplify their interpretation, I show results every six months for a straight line of fiber at offsets shorter than 200 meters responding to a virtual source at channel 75. These signals represent only Rayleigh wave arrival times (as opposed to the mix of Rayleigh and Love waves in Figure 3).

DISPERSION ANALYSIS

For each month I calculated the dispersion images for both types of NCF calculation, seen in Figure 5. The one-bit cross-correlation dispersion images split from 1-5 Hz into a higher and lower velocity. It is likely the higher velocity peak consistent with the coherence dispersion image (which is more robust to noise sources in the array)

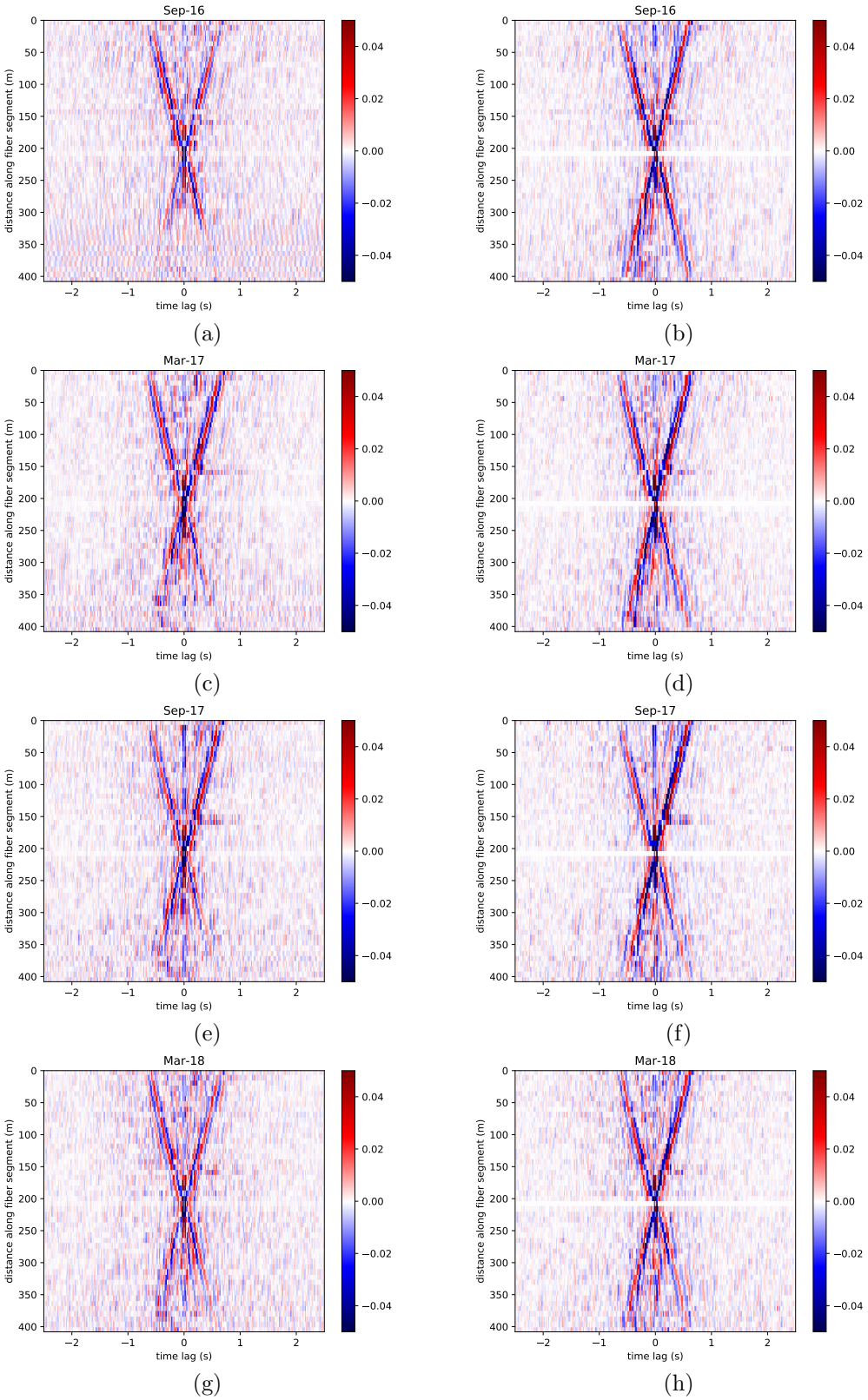

Figure 4: One-bit cross-correlations (left) and cross-coherences (right) of channel 75 with channels 50 to 100, at distances 0 to 400 meters, respectively, from the southwest corner of the array. From top to bottom: Sep. 2016, Mar. 2017, Sep. 2017, Mar. 2018. [**CR**]

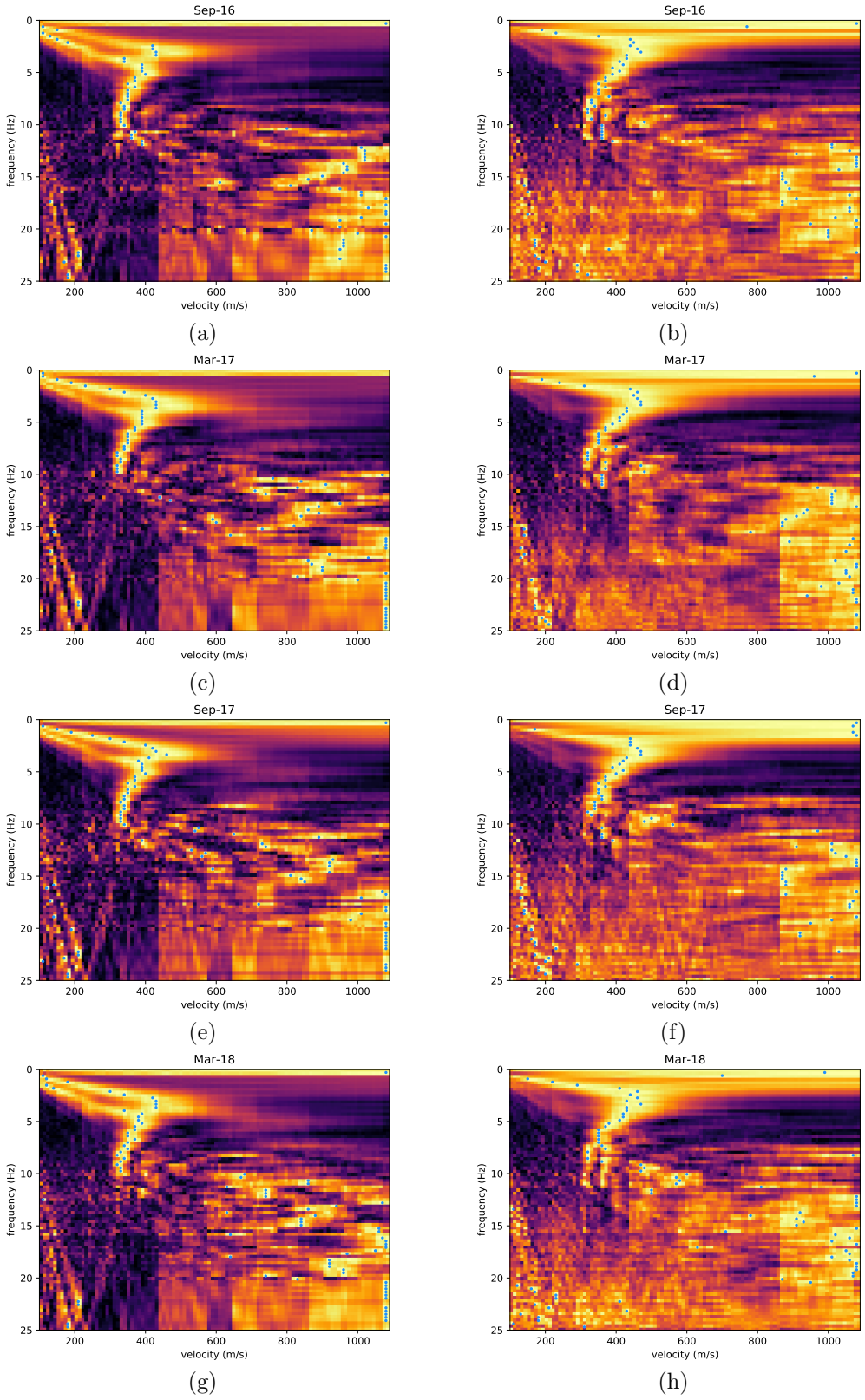

Figure 5: Dispersion images of monthly one-bit cross-correlations (left) and cross-coherences (right) in Figure 4. Yellow denotes more energy traveling at a particular frequency and velocity. Dark areas have less energy. Dots mark frequency-wise peak velocities. [**CR**]

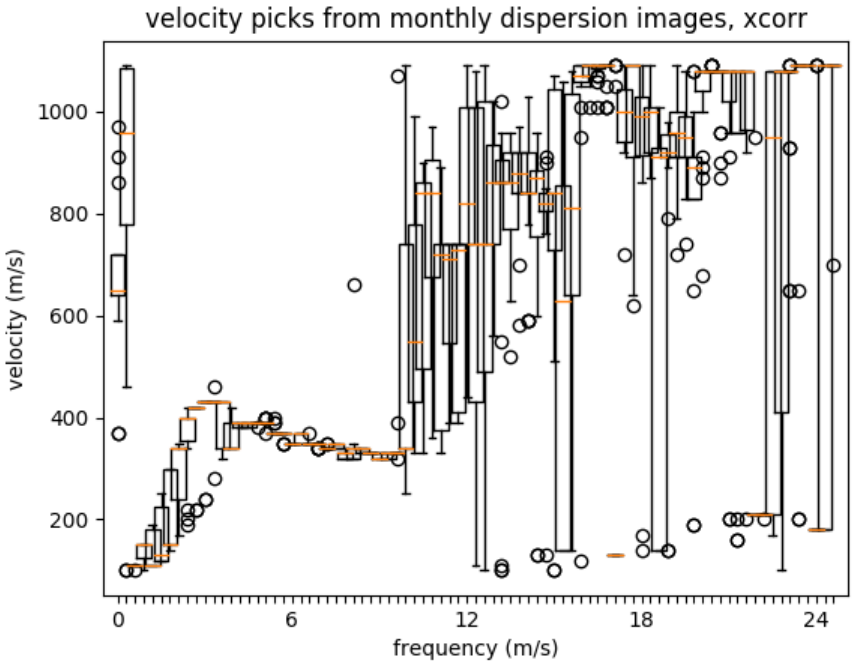

(a)

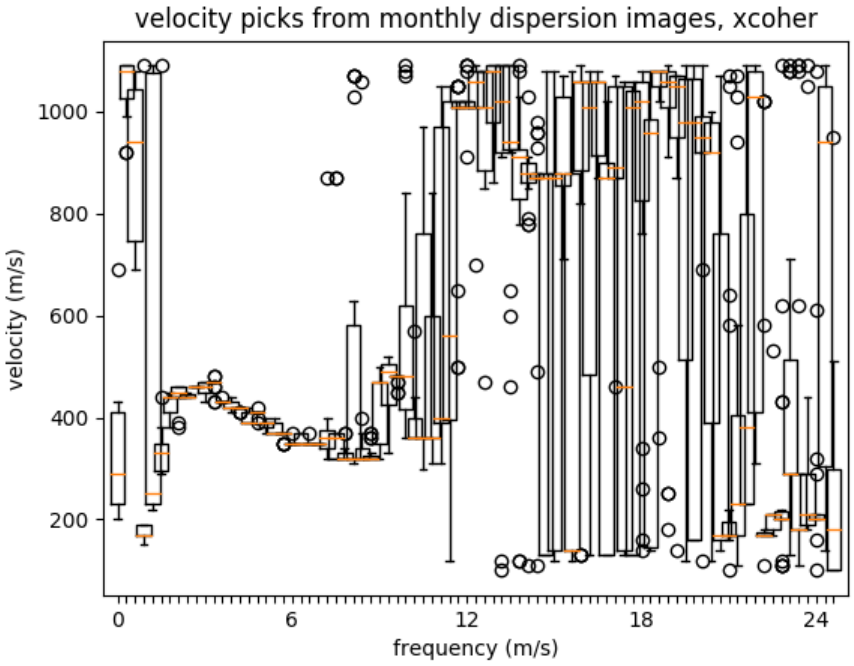

(b)

Figure 6: These box-and-whisker plots show the distribution of the channel 75 virtual source gathers' 18 monthly dispersion images' peak velocity picks for each frequency. This was repeated for both one-bit cross-correlation (top) and cross-coherence (bottom). [**CR**]

is reliable. The faster one-bit correlation peak is stronger and more consistent over all months, shown in Figure 6. There is not clear evidence of a velocity shift tied to saturation. Both types of dispersion image are coherent from 2-10 Hz, but vary at the high and low frequency ends by month (possibly due to changing noise levels), sometimes appearing to continue up to 12 Hz or down to 1 Hz. One-bit cross-correlations have more consistent dispersion curve picks in the 1-2 Hz range for more months than do cross-coherences. These picked velocities are typical of Rayleigh waves in geotechnical MASW studies, and given with the stability of these picks month-to-month this suggests ambient noise interferometry of DAS data is a reasonable tool for geotechnical surveys, even in urban areas.

A more complete picture of this variability can be seen when plotting the distribution of picks from monthly cross-coherences' dispersion images of multiple virtual source gathers. These distributions are seen in Figure 7 for virtual sources throughout the Via Ortega line (channels 55, 65, 75, 85, and 95, each approximately 80 m spaced), along with the distribution of each pick's wavelength versus frequency and wavelength versus velocity plots. These plots show very stable frequency versus wavelength curves for frequencies from 1 Hz up to 8-12 Hz, depending on the virtual source. In particular, channel 95 which is near the high traffic Campus Dr. and Via Ortega intersection is much less stable, showing a greater spread in the frequency/wavelength and frequency/velocity curves over time. While there is greater spread, it does not show any clear trend in summer versus winter months. at virtual sources on the south end (channels 55 and 65) there is a bit of a jump in wavelength at 6 Hz, suggesting a possible change around the area of parking structure 2 and Y2E2.

While the dispersion curves in Figure 7 are relatively coherent from 1 to 8-12 Hz for receiver pairs along Via Ortega, the virtual source gathers along the south side of the array, yield much less consistent dispersion picks. Figure 8 shows the same plots but for channels along the south edge of the array: channels 290 and 300 along Panama St. just south of Mitchell and Durand, channel 15 along Panama St. just south of Green building, and channels 25, 35, and 45 which are all between Roble and Arrillaga Gyms to the south of Panama St. In particular, channels 290 and 300 near Durand and Mitchell are particularly incoherent, even in the range of a few Hz. This may be an effect of being so close to the Durand and Mitchell basements, which cause large reverberations of vibrations, particularly seen during earthquakes. The rest of the virtual source locations seems to have some coherency in the 2-6 Hz range with wavelengths in the 50-150 meter range (so sensitive to thicknesses of 15-75 meters depth).

The dispersion curves for Rayleigh wave interferometry along the south side of the array are clearly less consistent than the curves for channels along Via Ortega. One possible explanation is that traffic on Panama St. and Campus Dr. would travel perpendicularly to Via Ortega, creating vibrations that would travel mostly parallel to Via Ortega (and thus be in the most sensitive zone for Rayleigh wave interferometry, yielding true Green's function velocities). Meanwhile that same traffic would travel mostly parallel to the south side of the array, creating waves that hit the southern

channels mostly broadside at angles outside the zone most important for Rayleigh wave interferometry. This is somewhat similar to difficulties encountered in the road-parallel line of the Richmond Field Station experiment (Dou et al., 2017). In theory, Rayleigh wave interferometry of a linear DAS array should be less effected by noises hitting the array broadside than a linear geophone array, so further experimentation should be done to determine whether this is the case at the Stanford Array.

CONCLUSIONS

I analyzed 18 months of ambient noise from a DAS array in an urban area. The data show large spatial variability, diurnal patterns, weekday/weekend patterns, and an annual winter increase in noise levels. Monthly one-bit cross-correlations show an SNR drop for NCFs in summer months, which may be a qualitative proxy for saturation (this deserves further investigation). One-bit cross-correlation dispersion images show two peaks 1-5 Hz, one of which continues from 1-10 Hz and is consistent with cross-coherence results that are more robust to non-ideal ambient noise, suggesting it is reliable. While this analysis does not show evidence of significant velocity change with seasonal rain patterns, the stability of these dispersion curves suggests DAS with careful noise analysis may be appropriate for urban geotechnical surveys in some urban areas, but this may depend in large part on fiber geometry relative to noise sources including roads.

ACKNOWLEDGEMENTS

During this project, Eileen Martin received funding from DOE CSGF under grant number DE-FG02-97ER25308, and the Schlumberger Innovation Fellowship, and Stanford Exploration Project affiliates. We thank Stanford IT for installing the fiber optic array, and Stanford SEEES IT for server room space and access. We thank OptaSense for their assistance in using the interrogator unit. We would also like to thank Jonathan Ajo-Franklin at Lawrence Berkeley National Lab and Nate Lindsey at University of California Berkeley for many useful discussions about time-lapse ambient noise interferometry with DAS data.

REFERENCES

Ajo-Franklin, J., S. Dou, N. Lindsey, T. Daley, B. Freifeld, E. Martin, M. Robertson, C. Ulrich, T. Wood, I. Eckblaw, and A. Wagner, 2017, Timelapse surface wave monitoring of permafrost thaw using distributed acoustic sensing and a permanent automated seismic source: Expanded Abstracts of the 87th SEG Ann. Internat. Mtg., 5223–5227.

Chang, J., S. de Ridder, and B. Biondi, 2016, High-frequency rayleigh-wave tomography using traffic noise from long beach, california: Geophysics, **81**, B43–B53.

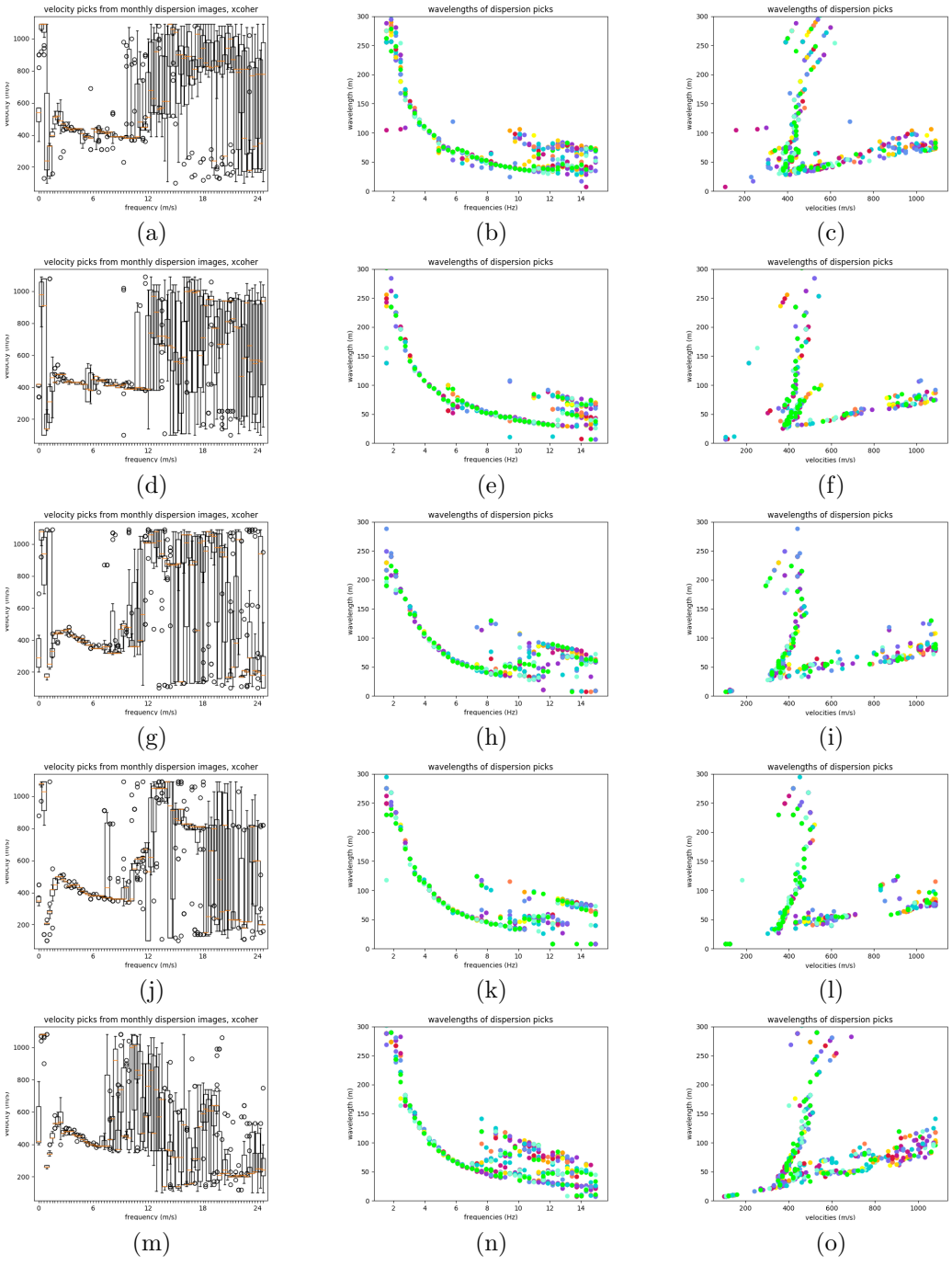

Figure 7: (Left) box plots of Rayleigh wave cross-coherence dispersion image picks, (center) corresponding picked wavelengths, and (right) velocities at those wavelengths plotted over all months (blues/greens are winter months, and reds/yellows are summer months) for virtual sources along Via Ortega at channels 55 (top), 65 (2nd row), 75 (3rd row), 85 (4th row) and 95 (bottom row). [**CR**]

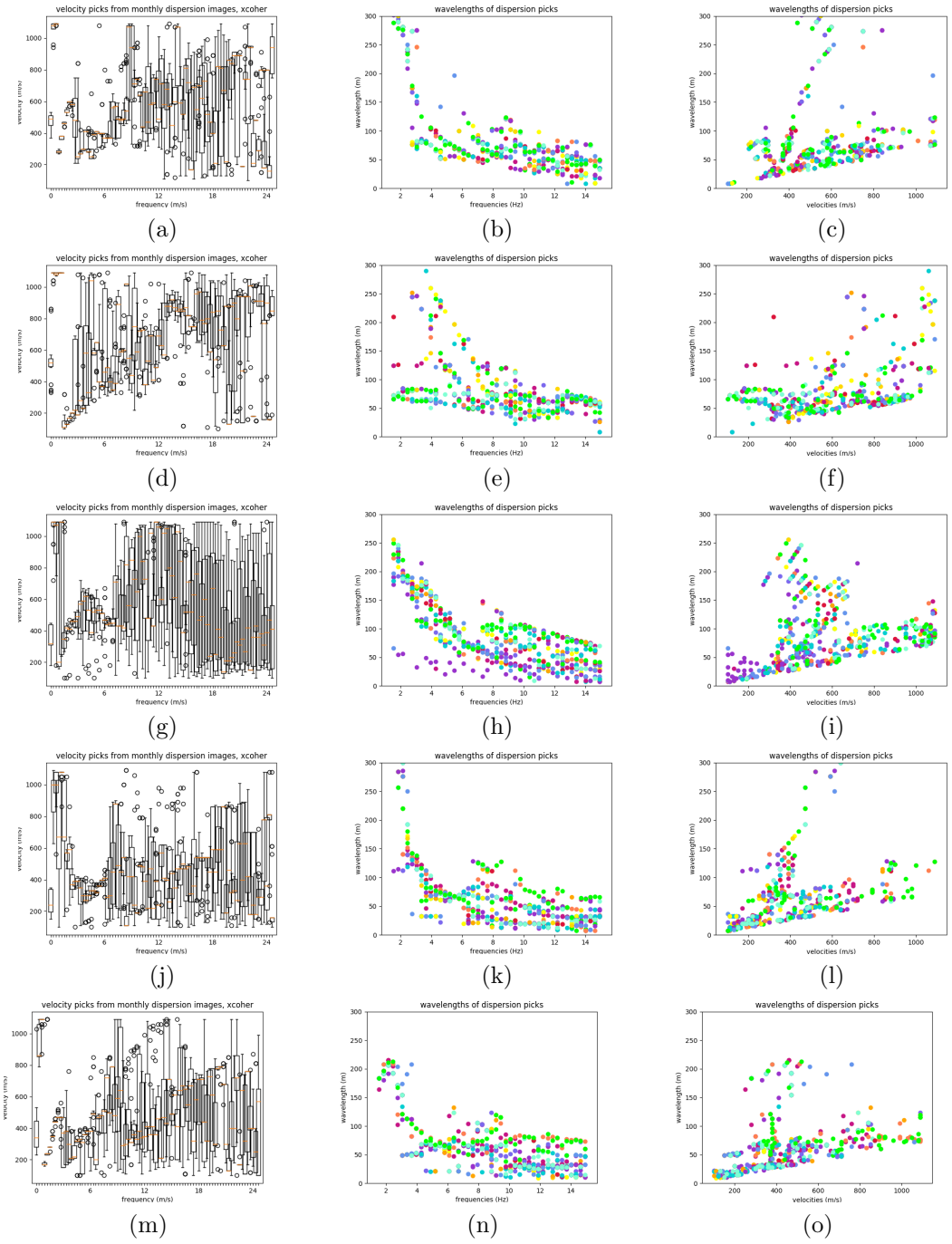

Figure 8: (Left) box plots of Rayleigh wave cross-coherence dispersion image picks, (center) corresponding picked wavelengths, and (right) velocities at those wavelengths plotted over all months (blues/greens are winter months, and reds/yellows are summer months) for virtual sources along the farthest south edge at channels 290 (top), 300 (2nd row), 15 (3rd row) every 10 channels to 35 (bottom row). [**CR**]

Clements, T. and M. Denolle, 2017, Observing drought-induced groundwater depletion in california with seismic noise: AGU Fall Meeting Abstract, S31A–0802.

Daskalakis, E., C. Evangelidis, J. Garnier, N. Melis, G. Papanicolaou, and C. Tsoga, 2016, Robust seismic velocity change estimation using ambient noise recordings: Geophysics Journal International, **205**, 1926–1936.

de Ridder, S., 2014, Passive seismic surface-wave interferometry for reservoir-scale imaging: PhD thesis, Stanford University.

Dou, S., N. Lindsey, A. Wagner, T. Daley, B. Freifeld, M. Robertson, J. Peterson, C. Ulrich, E. Martin, and J. Ajo-Franklin, 2017, Distributed acoustic sensing for seismic monitoring of the near surface: A traffic-noise interferometry example: Scientific Reports, **7**, article 11620.

Lindsey, N., S. Dou, E. Martin, A. Wagner, and J. Ajo-Franklin, 2017, 4-d permafrost thaw observations from ambient road traffic noise and a very dense distributed fiber optic sensing array: AGU Fall Meeting Abstract, S31A–0804.

Martin, E. and B. Biondi, 2017, Time-lapse changes in ambient noise interferometry and dispersion analysis at the stanford das array: Presented at the SEP Report 170.

Martin, E., C. Castillo, S. Cole, P. Sawasdee, S. Yuan, R. Clapp, M. Karrenbach, and B. Biondi, 2017, Seismic monitoring leveraging existing telecom infrastructure at the stanford distributed acoustic sensing array: Active, passive and ambient noise analysis: The Leading Edge, **36**, 1025–1031.

Martin, E., F. Huot, Y. Ma, R. Cieplicki, S. Cole, M. Karrenbach, and B. Biondi, 2018, A seismic shift in scalable acquisition demands new processing: Fiber-optic seismic signal retrieval in urban areas with unsupervised learning for coherent noise removal: IEEE Signal Processing Magazine, **35**, 31–40.

Martin, E., N. Lindsey, S. Dou, J. Ajo-Franklin, A. Wagner, K. Bjella, T. Daley, B. Freifeld, M. Robertson, and C. Ulrich, 2016, Interferometry of a roadside das array in fairbanks, ak: Expanded Abstracts of the 86th SEG Ann. Internat. Mtg., 2725–2729.

Zhan, Z., V. Tsai, and R. Clayton, 2013, Spurious velocity changes caused by temporal variations in ambient noise frequency content: Geophys. J. Int., **194**, 1574–1581.